Thermodynamics of a two-level system coupled to bosons

Raedt, Bart De; Raedt, Hans De

Published in:
Physical Review B

DOI:
10.1103/PhysRevB.29.5325

Publication date:
1984

Thermodynamics of a two-level system coupled to bosons

Bart De Raedt and Hans De Raedt
Physics Department, University of Antwerp, Universiteitsplein 1, B-2610 Wilrijk, Belgium
(Received 13 June 1983; revised manuscript received 19 December 1983)

We study the thermodynamic properties of a system described by two discrete energy levels, coupled to a bath of phonons. We derive a discrete path-integral representation for the partition function that is convenient for numerical evaluation and allows us to calculate in a unified manner the model properties in the whole coupling range. As a function of the coupling strength the system exhibits a transition from the weak-coupling regime to the self-trapped state. In the weak-coupling regime there is a periodic motion, similar to the tunneling of a particle in a double-well potential. In the strong-coupling regime, the periodicity is lost and the motion turns into a stochastic process.

I. INTRODUCTION

In this paper we present a detailed study of the thermodynamic properties of a two-level system coupled to a bath of phonons. The model Hamiltonian reads

$$H=-h\sigma^x+\sum_k[\omega_k a_k^+ a_k+\sigma^z(B_k a_k^+ +B_k^* a_k)]\ , \quad (1.1)$$

where σ^α denote the Pauli spin-$\frac{1}{2}$ matrices, satisfying $\sigma^\alpha\sigma^\beta=i\epsilon_{\alpha\beta\gamma}\sigma^\gamma$. This model may represent an impurity embedded in a crystal lattice. Then the first term gives the energy levels of the impurity in the absence of a coupling with the lattice modes. The second term represents the harmonic crystal and the third term is a bilinear coupling. Obviously (1.1) can only give a realistic description of the impurity if the thermal energy is smaller than the splitting of the lowest impurity levels ($T\lesssim 2h$) and if the energy of all other impurity levels is much larger than h, such that they can be neglected.

Model (1.1) is often used to describe the molecular polaron,[1–5] i.e., one electron that can be on either of the two sites on a molecule. The hopping motion of the electron is slowed down because the molecule interacts with the lattice vibrations. Hamiltonian (1.1) may model exciton-phonon systems,[2] spin-phonon relaxation,[6] paraelastic and paraelectric defects,[5–7] and rotational tunneling[8] in solids. It is closely related to the Wigner-Weiskopf-Dicke model in which a molecule interacts with the radiation field,[9] the only difference being that the coupling term (in the rotating-wave approximation) reads $\sigma^+ a_k+\sigma^- a_k^+$ instead of $\sigma^z(a_k+a_{-k}^+)$.

Under certain conditions it might be a reasonable approximation to replace the Hamiltonian of a particle moving in a double-well potential and interacting with a Gaussian bath by its projection onto the subspace spanned by the two lowest levels of the free particle and the boson Fock space. The resulting Hamiltonian is of the form (1.1) if one adds a term $\epsilon\sigma^z$ to allow for the general case of an asymmetric well.

From a theoretical viewpoint, the study of Hamiltonian (1.1) is important because it represents one of the simplest (but nontrivial) quantum models in which a particle (the spin) can exhibit substantially different behavior depending on the strength of the coupling to the external degrees of freedom (the phonons).

If there is no coupling to the phonons, and if at $t=0$ the spin is placed in the state $|\uparrow\rangle$, it will oscillate with frequency $2h$ between the states $|\uparrow\rangle$ and $|\downarrow\rangle$:

$$|\psi(t)\rangle=\cosh t\,|\uparrow\rangle-i\sinh t\,|\downarrow\rangle\ . \quad (1.2)$$

As long as the spin is only weakly coupled to the phonons the clocklike motion is still observed although damping will be present.[3–6] In the strong-coupling regime and at low temperatures, the effective tunneling rate is renormalized by an exponential factor[1–5] and if the coupling is larger than some critical value, the effective tunneling rate becomes so small that during the lifetime of an experiment, tunneling of the spin does not occur. Thus, even though there are two equivalent regions of phase space (spin up and down), the probability for the system to go from one region to the other is so small that the system is confined to only one region effectively.

If the first term in (1.1) is not present, the Hamiltonian is brought into diagonal form by the unitary transformation

$$U=\exp\left[\sum_k(a_k^+ +a_k)\frac{B^*(k)}{\omega_k}\sigma^z\right]\ , \quad (1.3a)$$

and can be written as

$$U^\dagger(H+h\sigma^x)U=\sum_k\omega^k a_k^+ a^k-C\ , \quad (1.3b)$$

$$C=\sum_k|B_k|^2/\omega_k\ , \quad (1.3c)$$

where C is the binding energy. From (1.3) it is clear that C is a measure of the strength of the coupling and therefore we will identify C with the coupling constant. Different methods, such as the WKB approximation,[1] time-dependent perturbation theory,[3] a mode-coupling scheme,[4,5] cumulant expansions,[6] and operator-ordering techniques,[10,11] have been used to study model (1.1).

We use the generalized Trotter formula[12,13] to derive a discrete path-integral representation of the partition function of the two-level system coupled to phonons. The

Trotter-formula approach is closely related to operator-ordering calculus, and as in Refs. 10 and 11 we find that evaluation of the partition function of spin-phonon model (1.1) can be reduced to the calculation of the partition function of a very peculiar one-dimensional (1D) Ising model with long-range interactions. The only difference between the 1D Ising model of Blume *et al.*[10,11] and ours is that our representation is well suited for numerical evaluation, independent of the strength of the coupling. This enables us to calculate accurately *all* relevant thermodynamic quantities.

In Sec. II we derive the discrete path integral for the partition function and we express thermodynamic properties in terms of the spins of the formally equivalent Ising model. In Sec. III we discuss the numerical methods. In Sec. IV we present our results and also make comparison with other work. Preliminary results have been reported elsewhere.[14]

II. THEORY

A. Discrete-path-integral formulation

In order to derive the discrete path integral for the partition function it is most convenient to use the coordinate representation for the phonons. Hamiltonian (1.1) may be rewritten as

$$H=-h\sigma^x+\sum_i \frac{p_i^2}{2M}+\tfrac{1}{2}\sum_{ij} V_{ij}x_i x_j+\sum_i \psi_i x_i \sigma^z , \tag{2.1}$$

and, without loss of generality, we may suppose the spin to be localized at the origin. If ψ_k denotes the Fourier transform of ψ_i, its relation to the coupling coefficient B_k in (1.1) reads

$$\psi_k=(2M\omega_k)^{1/2}B_k . \tag{2.2}$$

We use Trotter's formula to write for the partition function[12,13]

$$Z=\lim_{m\to\infty} Z_m , \tag{2.3a}$$

$$Z_m=\mathrm{Tr}(e^{-\tau H_1}e^{-\tau H_2}e^{-\tau H_3})^m , \tag{2.3b}$$

where $\beta=m\tau$ denotes the inverse temperature and where H_1, H_2, and H_3 represent the first, second, and two last terms of (2.1), respectively. We evaluate Z_m by inserting complete sets of states between its $3m$ factors. For the spin we work with the eigenstates of σ^z and for the phonons we use the coordinate representation. Within this representation H_3 is diagonal, but H_1 and H_2 are not. We identify each complete set by a greek subscript in contrast to roman indices that we use to label the lattice sites. If S_α denotes an Ising spin variable and $S_\alpha=\pm 1$ corresponds to the states "up" and "down," we may use the identities

$$\langle x_{i\alpha-1}|e^{-\tau p_i^2/2M}|x_{i\alpha}\rangle=\left[\frac{M}{2\pi\tau}\right]^{1/2}\times\exp\left[-\frac{M}{2\tau}(x_{i\alpha-1}-x_{i\alpha})^2\right] , \tag{2.4}$$

$$\langle S_{\alpha-1}|e^{\tau h\sigma^x}|S_\alpha\rangle=(\tfrac{1}{2}\sinh 2\tau h)^{1/2}\exp(JS_{\alpha-1}S_\alpha) , \tag{2.5a}$$

$$J=\tfrac{1}{2}\ln\coth\tau h , \tag{2.5b}$$

to obtain

$$Z_m=\left[\frac{M}{2\pi\tau}\right]^{Nm/2}(\tfrac{1}{2}\sinh 2\tau h)^{m/2}\times\int\{dx_{i\alpha}\}\sum_{\{S_\alpha\}}\exp(-S) ,$$
$$S=\sum_\alpha\left[-JS_{\alpha-1}S_\alpha+\tau\sum_i\psi_i x_{i\alpha}S_\alpha+\frac{M}{2\tau}\sum_i(x_{i\alpha-1}-x_{i\alpha})^2+\frac{\tau}{2}\sum_{ij}V_{ij}x_{i\alpha}x_{j\alpha}\right] . \tag{2.6}$$

It is now straightforward to integrate the phonons out and we find

$$Z_m=Z_m^P Z_m^S , \tag{2.7}$$

$$Z_m^P=\prod_{\alpha=1}^{m}\prod_{k\neq 0}\left[\tau^2\omega_k^2+2\left[1-\cos\frac{2\pi\alpha}{m}\right]\right]^{-1/2} , \tag{2.8}$$

$$Z_m^S=(\tfrac{1}{2}\sinh 2\tau h)^{m/2}\sum_{\{S_\alpha\}}\exp(-S_{\mathrm{eff}}) , \tag{2.9a}$$

$$S_{\mathrm{eff}}=-J\sum_{\alpha=1}^{m}S_{\alpha-1}S_\alpha-\tfrac{1}{2}\sum_{\alpha=1}^{m}\sum_{\gamma=1}^{m}F(\alpha-\gamma)S_\alpha S_\gamma , \tag{2.9b}$$

$$F(\alpha)=\tau^2\sum_k |B_k|^2 I_k(\alpha) , \tag{2.10}$$

$$I_k(\alpha)=\frac{2\tau\omega_k}{m}\sum_{\gamma=1}^{m}\left[\tau^2\omega_k^2+2\left[1-\cos\frac{2\pi\gamma}{m}\right]\right]^{-1}\cos\frac{2\pi\alpha\gamma}{m} . \tag{2.11}$$

The approximation Z_m has been factorized into a phonon part Z_m^P and a spin part Z_m^S. It is easily verified that $\lim_{m\to\infty}Z_m^P$ is the partition function of the free-phonon system. Therefore, in the limit $m\to\infty$, Z_m^S is the factor by which the partition function is changed due to the presence of the impurity.

The spin part Z_m^S is formally equivalent to the partition function of a chain of m Ising spins S_α with periodic boundary conditions. The spins interact through a nearest-neighbor coupling (related to the field h) and through an effective long-range interaction $F(\alpha-\gamma)$ originating from the phonons. However, because J depends on $\tau=\beta/m$ and $F(\alpha-\gamma)$ depends on β and m, one should be very careful in applying techniques developed for classical statistical problems to the evaluation of Z_m^S.[10,11] To demonstrate this point let us try to recover the (trivial) zero-coupling result $Z^S=2\cosh\beta h$ from (2.9). Because now we are dealing with a nearest-neighbor problem we can use the transfer-matrix method to obtain

$$Z_m^S=(\tfrac{1}{2}\sinh 2\tau h)^{m/2}(\lambda_+^m+\lambda_-^m) , \tag{2.12}$$

$$\lambda_\pm=(\coth\tau h)^{1/2}\pm(\tanh\tau h)^{1/2} , \tag{2.13}$$

TABLE I. Spin configurations for a chain of eight spins. Each configuration represents a class of N_c configurations, connected by symmetry. S_{eff} is the action corresponding to each configuration. The last column contains the total contribution to the partition function Z_m^S of all spin configurations connected by symmetry. The temperature $T/2h=0.1$, the coupling constant $C/2h=0.2$, and the frequency of the zone boundary phonon $\omega_D/2h=0.2$.

Spin configuration	Number of kinks	Multiplicity N_c	S_{eff}	$N_c\exp(-S_{\text{eff}})$
↑↑↑↑↑↑↑↑	0	2	−4.088	59.64
↑↑↑↑↑↑↑↓	2	16	−2.044	61.78
↑↑↑↑↑↑↓↓	2	16	−1.435	33.61
↑↑↑↑↑↓↓↓	2	16	−1.074	23.41
↑↑↑↑↓↓↓↓	2	8	−0.954	10.38
↑↑↑↑↑↓↑↓	4	16	−0.247	10.24
↑↑↑↑↓↑↑↓	4	16	−0.242	10.19
↑↑↑↓↑↑↑↓	4	8	−0.240	5.08
↑↑↑↑↓↑↓↓	4	32	0.120	14.19
↑↑↑↓↑↑↓↓	4	32	0.127	14.09
↑↑↑↓↑↓↓↓	4	16	0.242	6.28
↑↑↑↓↓↑↓↓	4	16	0.247	6.25
↑↑↓↑↑↑↓↓	4	4	0.254	1.55
↑↑↑↓↑↓↑↓	6	16	1.310	2.16
↑↑↓↑↑↓↑↓	6	16	1.314	2.15
↑↑↓↑↓↓↑↓	6	8	1.434	0.95
↑↑↓↑↓↑↓↓	6	16	1.435	1.90
↑↓↑↓↑↓↑↓	8	2	2.620	0.07

and we recover the exact result for each value of m: $Z_m^S=2\cosh\beta h$. However, even in the limit $m\to\infty$ we may not neglect the smaller eigenvalue λ_- in (2.12) as one is used to when dealing with a classical m-particle system. Because the long-range interaction $F(\alpha-\gamma)$ and the nearest-neighbor interaction J are positive, they both try to establish ferromagnetic order. Therefore, deviations from the ferromagnetic state are less likely to occur when the coupling gets stronger. Although S_{eff} is minimized by the totally ordered ferromagnetic state, this state does not correspond to the ground state of the quantum system. Again the reason for this lies in the dependence of J and $F(\alpha-\gamma)$ on β and m. In practice it is very difficult to say *a priori* which spin configurations (or paths) contribute to Z_m^S. To demonstrate this, we have given all spin configurations and their contribution to the partition function for a chain of eight spins in Table I. The temperature was taken as one tenth of the level splitting $2h$.

TABLE II. Contribution to the partition function Z_m^S of all spin configurations with the same number of kinks, for different values of the chain length: $m=2,\ldots,8$. The other model parameters are the same as in Table I.

Number of kinks	0	2	4	6	8
$m=2$	2.61	0.38			
$m=3$	4.03	1.88			
$m=4$	6.00	5.24	0.43		
$m=5$	9.49	12.08	2.40		
$m=6$	16.25	26.39	8.39	0.22	
$m=7$	30.04	57.63	24.71	1.60	
$m=8$	59.64	129.18	67.88	7.17	0.07

For the meaning of the other model parameters, which is not so important for the moment, we refer to Sec. III. In the first column we show a spin configuration which is representative for all configurations that make the same contribution to Z_m^S. The other configurations are easily found by using symmetry relations. In the second column we give the total number of kinks in the chain for the given configuration. Because of the periodic boundary conditions this is always an even number. The third and the fourth column give the multiplicity N_c and the "action" S_{eff} for that spin configuration. In the last column we give the total contribution to the partition function Z_m^S of all configurations connected by symmetry. It is easily seen that configurations with two kinks give the largest contribution, followed by four-kink configurations and only then by the totally ordered configuration. In Table II one may follow the evolution of the different contributions when the number of time slices m is varied. It will be obvious to the reader that when m is increased further (which would be necessary to obtain reliable results at this low temperature), configurations with more kinks will become important also. Thus the high multiplicity of such states compensates for their larger action. From these observations we conclude that in general it is impossible to restrict the spin sum to certain configurations.

B. Thermodynamic quantities

From (2.7)–(2.11) it is straightforward to calculate approximations for thermodynamic quantities of the system described by Hamiltonian (1.1). As an example we consider the free energy: the approximation F_m (for finite m) for the free energy $F=F_\infty$ is given by $F_m=F_m^P+F_m^S$

with $F_m^P=-\beta^{-1}\ln Z_m^P$ and $F_m^S=-\beta^{-1}\ln Z_m^S$. As the calculation of Z_m^P from (2.8) is trivial we only have to concentrate on the evaluation of Z_m^S and its related thermodynamic quantities. The expressions for the approximations to the magnetization $\langle\sigma^x\rangle$, the susceptibilities χ^x, χ^y, and χ^x and the (spin) energy E^S are summarized as follows:

$$\langle\sigma^x\rangle_m=h\chi_m^y=(\cosh 2\tau h-\langle S_\alpha S_{\alpha+1}\rangle)/\sinh 2\tau h\ , \tag{2.14}$$

$$\chi_m^x=\tau\,\mathrm{csch}^2 2\tau h\left[\sum_\alpha(\langle S_\alpha S_{\alpha+1}S_\gamma S_{\gamma+1}\rangle-\langle S_\alpha S_{\alpha+1}\rangle^2)+2(\cosh 2\tau h\langle S_\alpha S_{\alpha+1}\rangle-1)\right], \tag{2.15}$$

$$\chi_m^x=\tau\sum_\alpha\langle S_\gamma S_{\gamma+\alpha}\rangle\ , \tag{2.16}$$

$$E_m^S=-h\langle\sigma^x\rangle_m-\frac{1}{2m}\sum_\alpha\sum_\gamma\frac{\partial F(\alpha-\gamma)}{\partial\tau}\langle S_\alpha S_\gamma\rangle\ . \tag{2.17}$$

In Eqs. (2.14)—(2.17), expectation values of Ising spins $\langle\cdots S_\alpha\cdots\rangle$ are defined by the probability distribution $\exp(-S_{\mathrm{eff}})$ for a given m value. Two more quantities are of special interest for the study of the transition between the weak- and strong-coupling regime. As already mentioned, the constant C, given by (1.3c), is a measure of the strength of the spin-phonon coupling. The derivative of the free energy with respect to C is the expectation value of the coupling term of the Hamiltonian:

$$\frac{\partial F}{\partial C}=\frac{1}{2C}\langle H_c\rangle,\quad H_c=\sum_k(B_k a_k^+ +B_k^* a_k)\sigma^z\ . \tag{2.18}$$

The second derivative,

$$\frac{\partial^2 F}{\partial C^2}=-\frac{1}{4C^2}\left[\int_0^\beta d\lambda\langle e^{\lambda H}H_c e^{-\lambda H}H_c\rangle-\beta\langle H_c\rangle^2+\langle H_c\rangle\right], \tag{2.19}$$

is a measure for the fluctuation of the coupling energy, the first two terms of (2.19) correspond to the susceptibility of H_c. To derive (2.18)—(2.19), one may note from (1.3c) that B_k can be rewritten as $C^{1/2}A_k$, where $\partial A_k/\partial C=0$. In terms of the Ising spins the corresponding approximations read

$$\frac{\partial F_m}{\partial C}=-\frac{1}{2\beta}\sum_\alpha\sum_\gamma\frac{\partial F(\alpha-\gamma)}{\partial C}\langle S_\alpha S_\gamma\rangle\ , \tag{2.20}$$

$$\frac{\partial^2 F_m}{\partial C^2}=-\frac{1}{4\beta}\left\langle\left[\sum_\alpha\sum_\gamma\frac{\partial F(\alpha-\gamma)}{\partial C}S_\alpha S_\gamma\right]^2\right\rangle+\beta\left[\frac{\partial F_m}{\partial C}\right]^2. \tag{2.21}$$

Regarding the last formula we remark that $\partial^2 F(\alpha-\gamma)/\partial C^2=0$.

C. Special limits

According to (2.3a) $\lim_{m\to\infty}Z_m^S$ is the quantity we want to calculate. If m is sufficiently large, such that $\tau h\ll 1$ and $\tau\max(\omega_k)\ll 1$, we have

$$J\to-\tfrac{1}{2}\ln\tau h,\quad \tfrac{1}{2}\sinh 2\tau h\to\tau h\ , \tag{2.22a}$$

$$I_k(\alpha)\to(e^{-\tau\omega_k|\alpha|}+e^{-\tau\omega_k(m-|\alpha|)})(1-e^{-\beta\omega_k})^{-1}\ , \tag{2.22b}$$

and obtain

$$Z_m^S=\sum_{\{S_\alpha\}}\prod_{\alpha,\gamma=1}^m\exp\left[\frac{1-S_\alpha S_{\alpha+1}}{2}\ln\tau h+\tau^2\sum_k|B_k|^2 I_k(\alpha-\gamma)S_\alpha S_\gamma\right], \tag{2.22c}$$

which is exactly the expression derived by Blume *et al.*[10] In general, neither (2.22) nor (2.9) can be solved rigorously. As we will compute the temperature-dependent spin properties of extrapolating numerical results obtained from the finite-m approximants Z_m^S, it is more expedient to use the genuine finite-m expression (2.9) instead of the limiting form (2.22) because we will get more accurate answers. This is most easily seen by considering the noninteracting case $B_k=0$. As we pointed out in Sec. II, (2.9) will give us the rigorous result for any value of m whereas from (2.22) we only recover the exact answer if we explicitly take the limit $m\to\infty$.[10,11]

Another special case which is important is the adiabatic limit. Operationally, taking this limit is equivalent to neglecting the kinetic energy of the oscillators. In terms of the discrete path integral this implies that we should multiply the integrand in (2.6) by $\prod_{\alpha=1}^{m-1}\delta(x_{i\alpha}-x_{i\alpha+1})$ and we obtain

$$Z_m^S=(\tfrac{1}{2}\sinh 2\tau h)^{m/2}\sum_{\{S_\alpha\}}\exp(-S_{\mathrm{eff}})\ , \tag{2.23a}$$

$$S_{\mathrm{eff}}=-J\sum_{\alpha=1}^m S_{\alpha-1}S_\alpha-\frac{\beta C}{m^2}\sum_{\alpha=1}^m\sum_{\gamma=1}^m S_\alpha S_\gamma\ . \tag{2.23b}$$

Thus we see that in the adiabatic limit the effective long-range interaction is independent of the distance between the spins. Furthermore, the strength of this effective coupling does not depend on the details of the phonon energy ω_k and spin-phonon coupling B_k. In particular, the dimensionality of the phonon system plays no role.

An appealing feature of the adiabatic model is that it can be solved exactly.[4,5,15] Of special interest are the ground-state properties. One finds[4,5]

$$E_g=\begin{cases}-h, & C<h/2\\ -C[1+(h/2C)^2], & C>h/2,\end{cases} \tag{2.24a}$$

$$\langle\sigma^z\rangle=\begin{cases}0, & C<h/2\\ [1-(h/2C)^2]^{1/2}, & C>h/2,\end{cases} \tag{2.24b}$$

$$\chi^z=\begin{cases}1/h-2C, & C<h/2\\ h^2/2C(4C^2-h^2), & C>h/2,\end{cases} \tag{2.24c}$$

$$-\frac{\partial^2 E_g}{\partial C^2}=\begin{cases}0, & C<h/2\\ h^2/8C^3, & C>h/2.\end{cases} \tag{2.24d}$$

From (2.24) we conclude that in the adiabatic limit, model (1.1) exhibits a ground-state phase transition at $C=h/2$. The susceptibility χ^z diverges if $C\to 2h$ and there is a discontinuity in the second derivative of the (free) energy with respect to the coupling C. Furthermore, the nature of the transition does not depend on the precise form of ω_k or B_k but only on the binding energy $C=\sum_k |B_k|^2/\omega_k$. For $T>0$ the sharp transition as described by (2.24) will be smoothed by thermal fluctuations.

III. NUMERICAL EVALUATION

Until now our discussion of the two-level system was quite general. To proceed further it is necessary to specify the model parameters completely. We choose the level splitting $2h$ of the uncoupled system as the energy unit. The system is then characterized by three parameters: the temperature $T/2h$, the coupling $C/2h$, and the maximum (or cutoff) of the phonon frequency $\omega_D/2h$, but of course there is still a large freedom of choice for the explicit form of ω_k and B_k. For a one-dimensional lattice we take

$$\omega_k=\omega_D\,|\sin(k/2)|\ , \tag{3.1a}$$

$$B_k=i(C\omega_D^2\sin^2 k/2\omega_k N)^{1/2}\ , \tag{3.1b}$$

and in three dimensions we consider isotropic Debye phonons

$$\omega_k=ck\ , \tag{3.2a}$$

$$B_k=i(C\omega_k/N)^{1/2}\ . \tag{3.2b}$$

Here N is the number of lattice sites. It is easy to verify that (3.1) and (3.2) satisfy (1.3c).

Having discussed the relevant parameters, we turn to the question of convergence of the approximations (2.14)—(2.17) and (2.20)—(2.21) as a function of the number of "time slices" m. In general, for any set of parameters, one should study the approximations as a function of $1/m$. We already demonstrated in Sec. II that for $C=0$ the exact results are reproduced for any m value. Therefore, we expect that the m value required to obtain a certain accuracy to increase with increasing C. Also the imaginary time step $\tau=\beta/m$ must be sufficiently small, and consequently the required m value will become larger with lower temperature. Moreover the convergence rate will be different for different thermodynamic quantities. In Fig. 1 we show the energy E_m^S for $T/2h=0.1$ and $\omega_D/2h=2$ as a function of the coupling for $m=5$, 10, 20, 40. Because the temperature is very low in this case we need relatively high m values in order to make τ small enough. We observe that $E_m^S<E_n^S<E^S$ for $m<n<\infty$. Thus the energy converges from below, and we also see that convergence is slower for larger C values as anticipated. In Fig. 2 we focus on the $1/m$ dependence of E_m^S and $\partial^2 F_m/\partial C^2$ for $C/2h=0.5$, $\omega_D/2h=2$, and $T/2h=0.1,0.2$. We clearly see that convergence is faster for higher temperature as expected. For $T/2h=0.2$, $m=20$ gives already accurate results for both quantities, whereas for $T/2h=0.1$ we must go to $m=40$ for the same accuracy. This is not surprising because when the temperature is two times smaller we must double m to obtain the same τ value.

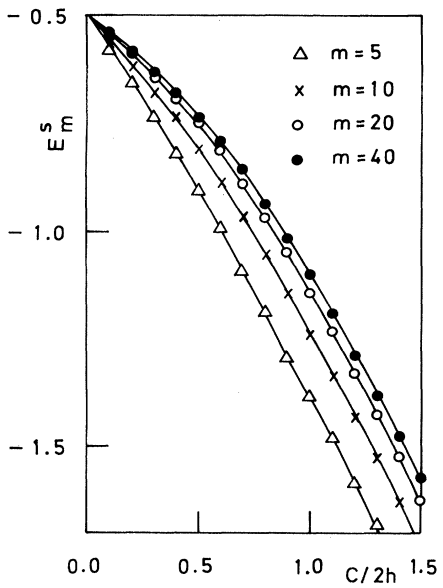

FIG. 1. The approximation E_m^S for the energy, for different values of the number of "imaginary time slices" m, as a function of the coupling strength C (in units of the level splitting $2h$). The temperature $T/2h=0.1$ and the phonon cutoff frequency $\omega_D/2h=2$.

The numerical procedures to calculate the thermodynamics are straightforward. For m values up to $m=20$, the sum over the spin states in (2.9) can easily be performed exactly by today's computers as the total number of states then equals $2^{20}\approx 10^6$. For a large region of the parameter space this has proven to be sufficient. Thus results presented here for $m\leq 20$ are numerically exact. For very low temperatures it is necessary to go to higher m values in order to make τ sufficiently small. Then we use the well-known Monte Carlo simulation technique.[16] Because (2.9) looks like the partition function of an Ising

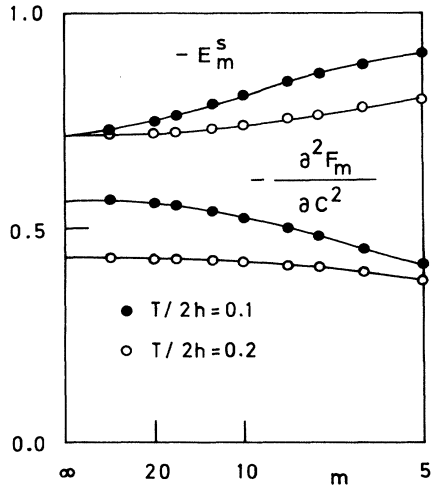

FIG. 2. Demonstration of the convergence of results for the energy and the fluctuation of the coupling term as a function of $1/m$. The coupling $C/2h=0.5$ and the phonon cutoff frequency $\omega_D/2h=2$. Convergence is faster for higher temperature T.

model, we can use the classical method without any restriction. Data produced in this way have statistical errors due to the Monte Carlo sampling. The error is proportional to $N_S^{-1/2}$, where N_S is the number of samples taken in the Monte Carlo process. For our data we used 10 000 samples per spin to allow the system to reach thermal equilibrium and 50 000 samples per spin for calculating averages.

IV. RESULTS

In Figs. 3—10 we present extensive numerical results for $\omega_D/2h=0.2$, which corresponds to a zone-boundary phonon with a frequency smaller than the level splitting $2h$. The results presented in Figs. 3—10 are extrapolations of data for $m \leq 20$ to $m=\infty$ (as done in Fig. 2) and therefore they correspond to the exact values, apart from small errors due to the extrapolation. We have found no qualitative and only tiny quantitative differences between 1D and 3D systems as is demonstrated in Table III. The reason for this is that we are still close to the adiabatic regime in which the results only depend on two dimensionless parameters $C/2h$ and $T/2h$ (see Sec. II C). However, if we compare the adiabatic result for the transition value of the coupling $C/2h=0.25$ with the position of the maximum of $-\partial^2 F/\partial C^2$ at low temperature $C/2h \sim 0.4$ (cf. Fig. 10), we already observe a deviation from the adiabatic result. This effect may not be attributed to the fact that our calculations are for nonzero temperatures, because we find a shift of the maximum to higher C with decreasing T.

In Figs. 3—6 we study the temperature dependence in the region $0.1 \leq T/2h \leq 1$ for several values of the coupling constant C. In Fig. 3 we show the (spin) energy E^S. It is remarkable that for sufficiently strong coupling, E^S first decreases and then increases with increasing temperature. This corresponds to a negative (spin) specific heat. Obviously the total specific heat of the system is always positive. The reason for this anomaly can be understood as follows. At very low temperature only $k \approx 0$ phonons are present. With increasing temperature, the presence of higher k phonons allows the spin to build a favorable local field and thus to lower its energy. At still higher T all phonon modes are highly excited and E^S starts to increase again. In Fig. 4 the magnetization $\langle \sigma^x \rangle$ is shown. For

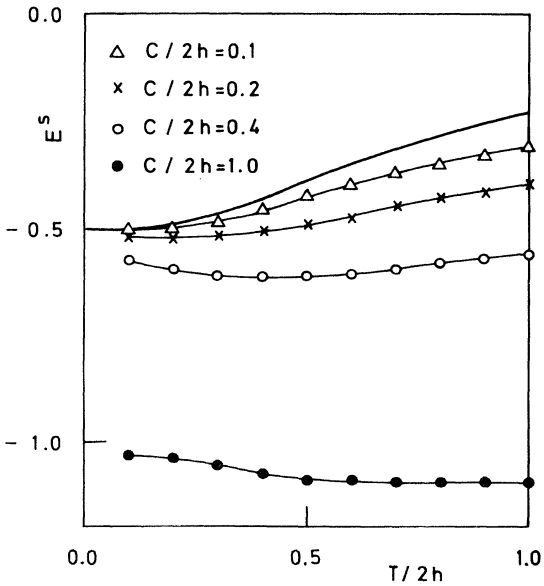

FIG. 3. Temperature dependence of the (spin) energy E^S for different values of the coupling C. The solid line is the exact zero-coupling result. The phonon cutoff frequency $\omega_D/2h=0.2$.

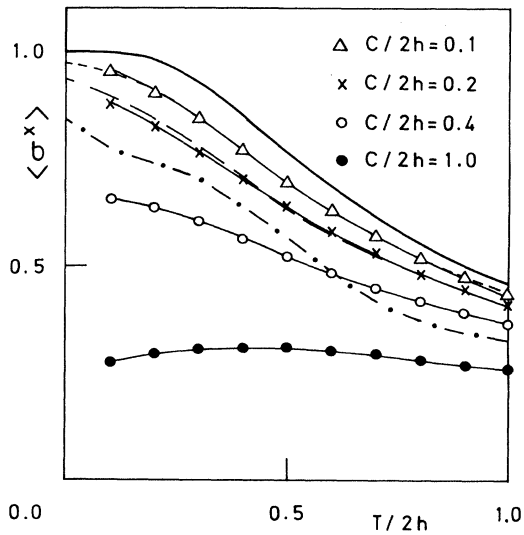

FIG. 4. Temperature dependence of the magnetization $\langle \sigma^x \rangle$ for different values of the coupling C. The solid line is the exact zero-coupling result. The phonon cutoff frequency $\omega_D/2h=0.2$. Also shown are the results of the mode-coupling theory given in Ref. 5. Short dashes: $C/2h=0.1$; long dashes: $C/2h=0.2$; and dashed-dotted line: $C/2h=0.4$.

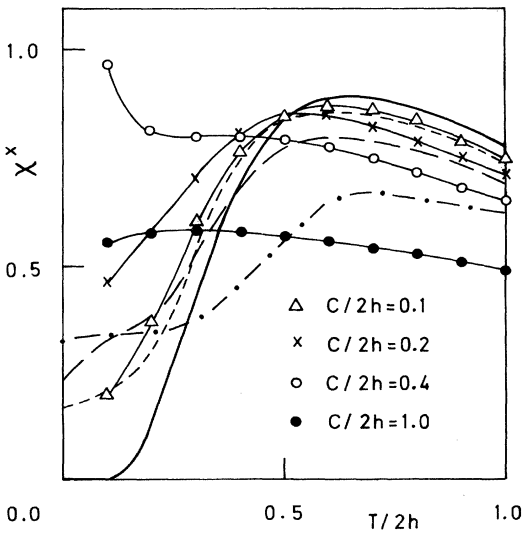

FIG. 5. Temperature dependence of the transverse susceptibility χ^x for different values of the coupling C. The solid line is the exact zero-coupling result. The phonon cutoff frequency $\omega_D/2h=0.2$. Mode-coupling results of Ref. 5 are given by the dashed lines, using the same convention as in Fig. 4.

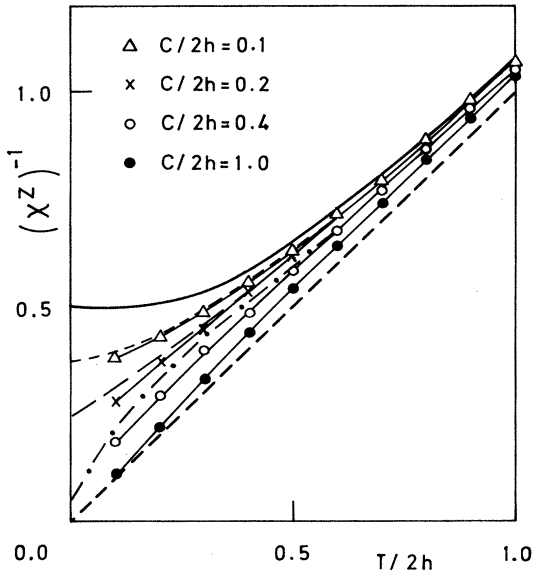

FIG. 6. Temperature dependence of the inverse longitudinal susceptibility $(\chi^z)^{-1}$ for different values of the coupling C. The solid line is the exact zero-coupling result. The phonon cutoff frequency $\omega_D/2h=0.2$. Mode-coupling results of Ref. 5 are given by the dashed lines using the same convention as in Fig. 4.

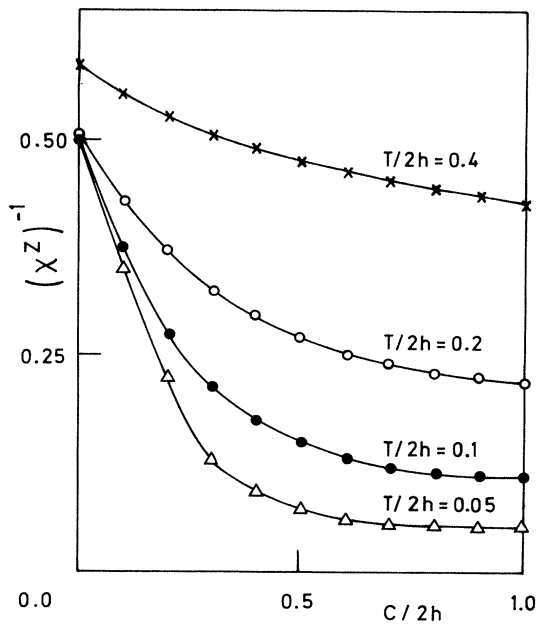

FIG. 8. Coupling dependence of the inverse longitudinal susceptibility $(\chi^z)^{-1}$ for different values of the temperature T. Results for $T/2h=0.4,0.2,0.1$ are extrapolations of exact numerical data for $m=2,\ldots,20$ to $m=\infty$. Results for $T/2h=0.05$ are Monte Carlo data for $m=100$. The phonon cutoff frequency $\omega_D/2h=0.2$.

weak coupling, $\langle\sigma^x\rangle$ behaves qualititively the same as for $C=0$; it decreases monotonically with T. For strong coupling the magnetization exhibits a broad maximum. Figure 5 displays the transverse susceptibility χ^x. For high T, χ^x decreases when the coupling gets stronger. For low T, χ^x has a maximum as a function of C around $C/2h\approx 0.4$. In Fig. 6 we have plotted the inverse longitudinal susceptibility $(\chi^z)^{-1}$. For large values of C, χ^z obeys the Curie law asymptotically in the low-temperature as well as in the high-temperature limit. This would mean a divergent χ^z at $T=0$ for strong coupling. In the weak-coupling regime, χ^z obeys the Curie law for $T\to\infty$, but it approaches a finite value for $T=0$. The results presented up to now already indicate that the two-level system

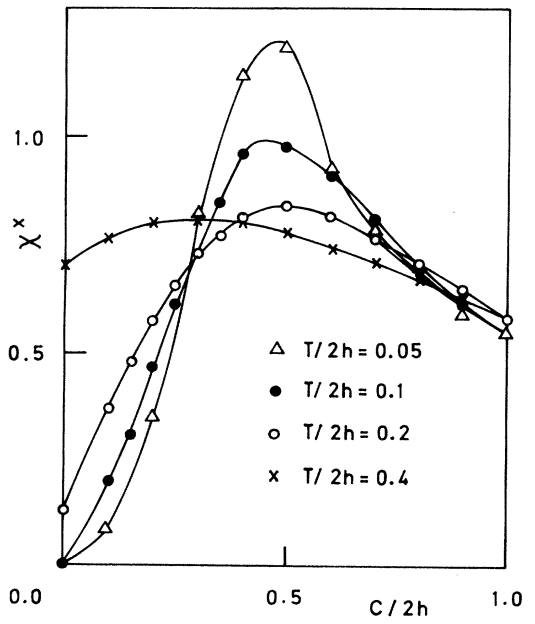

FIG. 7. Coupling dependence of the transverse susceptibility χ^x for different values of the temperature T. Results for $T/2h=0.4$, 0.2, 0.1 are extrapolations of exact numerical data for $m=2,\ldots,20$ to $m=\infty$. Results for $T/2h=0.05$ are Monte Carlo data for $m=100$. The phonon cutoff frequency $\omega_D/2h=0.2$.

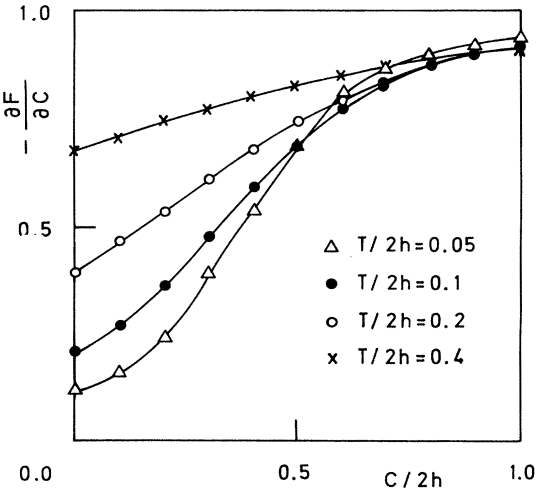

FIG. 9. Coupling dependence of the expectation value of the coupling term of the Hamiltonian $\partial F/\partial C$ for different values of the temperature T. Results for $T/2h=0.4,0.2,0.1$ are extrapolations of exact numerical data for $m=2,\ldots,20$ to $m=\infty$. Results for $T/2h=0.05$ are Monte Carlo data for $m=100$. The phonon cutoff frequency $\omega_D/2h=0.2$.

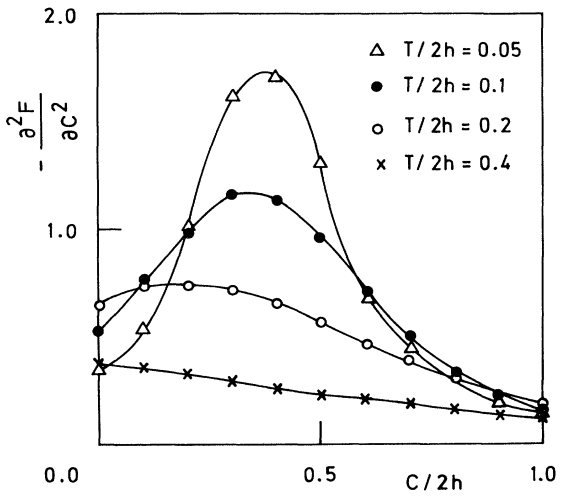

FIG. 10. Coupling dependence of the fluctuation of the coupling energy [cf. Eq. (2.19)], for different values of the temperature T. Results for $T/2h=0.4,0.2,0.1$ are extrapolations of exact numerical data for $m=2,\ldots,20$ to $m=\infty$. Results for $T/2h=0.05$ are Monte Carlo data for $m=100$. The phonon cutoff frequency $\omega_D/2h=0.2$.

behaves quite different, depending on the strength of the coupling. In Figs. 7—10 we give results for the transverse and (inverse) longitudinal susceptibility, for the coupling energy $\partial F/\partial C$ and for $\partial^2 F/\partial C^2$, which is a measure for the fluctuation of the coupling energy. (Note that in these figures the results for $T/2h=0.05$ are Monte Carlo data for $m=100$.) In all these quantities a transition for $C/2h\approx 0.4$ clearly shows up, and the transition region becomes smaller at lower temperatures. This suggests that, as for the adiabatic case, there may be a discontinuity in the ground state of the system as a function of C. Our method only allows us to obtain results down to very low temperatures; we cannot provide definite answers about the system for $T=0$. Moreover $T=0$ is not necessarily the same as $T\to 0$ in which case we consider the former as of academic interest only.

In order to elucidate the nature of the transition we now turn to a discussion of the dynamical behavior of the system. As we pointed out in the Introduction, for $C=0$ the spin motion is equivalent to the motion of a particle in a double-well potential (if we may restrict ourselves to the two lowest levels), the eigenstates of σ^x being the exact energy eigenstates of the system. On the other hand, the eigenstates of σ^z correspond to states in which the particle is localized in one of the potential wells, and tunneling through the potential barrier corresponds to an oscillation between those states. To see how this motion is modified by the coupling to the phonons we study the dynamic relaxation function $\Phi_z(t)$. For $C=0$ we find

$$\Phi_z(t)=h^{-1}\tanh\beta h\cos 2ht=\chi^z\cos 2ht\ , \tag{4.1}$$

and this describes an undamped oscillation with frequency $2h$ at any temperature. For nonzero coupling we make use of the continued fraction representation for the Laplace transform of the relaxation function and the knowledge of the frequency moments. Formally we can write[17]

$$\Phi_z(z)=\cfrac{\chi^z}{z-\langle\omega^2\rangle/[z-(\langle\omega^4\rangle/\langle\omega^2\rangle-\langle\omega^2\rangle)/(z-\cdots)]},\quad z=\omega+i\epsilon \tag{4.2a}$$

with

$$\langle\omega^2\rangle=(\chi^z)^{-1}\langle[\sigma^z,[H,\sigma^z]]\rangle\ , \tag{4.2b}$$

$$\langle\omega^4\rangle=(\chi^z)^{-1}\langle[[H,\sigma^z],[H,[H,\sigma^z]]]\rangle\ . \tag{4.2c}$$

For $C=0$, $\langle\omega^2\rangle=4h^2$ and $\langle\omega^4\rangle=\langle\omega^2\rangle^2$ and therefore (4.2a) reduces to $\Phi_z(z)=\chi^z z(z^2-4h^2)^{-1}$, which is the Laplace transform of (4.1). For nonzero coupling we can evaluate the frequency moments and we find

$$\langle\omega^2\rangle=4h\langle\sigma^x\rangle(\chi^z)^{-1}\ , \tag{4.3a}$$

$$\langle\omega^4\rangle=16h^2(\langle\sigma^x\rangle-2C\,\partial F/\partial C)(\chi^z)^{-1}\ . \tag{4.3b}$$

Consequently the continued fraction does not terminate at the second step as for the $C=0$ case. Now we use a three-pole approximation to terminate (4.2a):[18]

TABLE III. Comparison of results for a two-level system coupled to one- and three-dimensional phonons for three values of the coupling constant C. The temperature $T/2h=0.1$, the number of "imaginary time slices" $m=20$, and the frequency of the zone boundary phonon $\omega_D/2h=0.2$.

$C/2h$	0.1	0.1	0.4	0.4	1	1
d	1	3	1	3	1	3
E_m^S	−0.505	−0.508	−0.589	−0.594	−1.114	−1.114
$\langle\sigma^x\rangle_m$	0.951	0.951	0.685	0.689	0.335	0.337
χ_m^x	0.198	0.194	0.908	0.896	0.634	0.637
χ_m^z	2.734	2.719	6.057	5.981	9.452	9.436
$\partial F_m/\partial C$	−0.281	−0.290	−0.609	−0.607	−0.946	−0.944
$\partial^2 F_m/\partial C^2$	−0.806	−0.774	−1.168	−1.143	−0.154	−0.157

$$\Phi_z(z)=\frac{\chi^z}{z-\langle\omega^2\rangle/\{z-(\langle\omega^4\rangle/\langle\omega^2\rangle-\langle\omega^2\rangle)/[z+i(\langle\omega^4\rangle/\langle\omega^2\rangle)^{1/2}]\}} . \tag{4.4}$$

It can be verified that the spectral response $\Phi_z''(\omega)$, corresponding to (4.4), satisfies the second and fourth frequency sum rule.[18] Because we have evaluated the static quantities appearing in (4.3), we can determine the spectrum from (4.4) for any C value. For small coupling we find a shift and a broadening of the resonances located near $2h$, but qualitatively the spectrum is similar to the $C=0$ spectrum. Thus the oscillatory motion is still retained, although there is some damping and a frequency shift due to the spin-phonon coupling. Let us now see what happens for $T\to 0$ and strong coupling. Then $\chi^z\approx 1/T$ and thus $\langle\omega^2\rangle\approx 0$. Therefore, the spectrum will consist of a very narrow peak centered around $\omega=0$. Equation (4.4) then simplifies to

$$\Phi_z(z)=\frac{\chi^z}{z+i\lambda} , \tag{4.5a}$$

and the width is given by

$$\lambda=\langle\omega^2\rangle^{3/2}/\langle\omega^4\rangle^{1/2} . \tag{4.5b}$$

Here we remark that because σ^z commutes with the spin-phonon interaction term of the Hamiltonian, our problem is very similar to motional narrowing in magnetic resonance, and the result (4.5b) obtained for the linewidth is the same.[19] When C is much larger than the "critical" coupling value and in the limit of low temperatures we may estimate λ by putting $\chi^z\approx 1/T$, $\partial F/\partial C\approx 1$, and $\langle\sigma^x\rangle\sim 1/C$. (In order to really satisfy these relations one must go to C values higher than those presented in the figures, but Figs. 4, 6, 8, and 9 are sufficient to make them plausible.) Thus we find

$$\lambda\sim T/C^2,\quad T\to 0,\ C\to\infty . \tag{4.6}$$

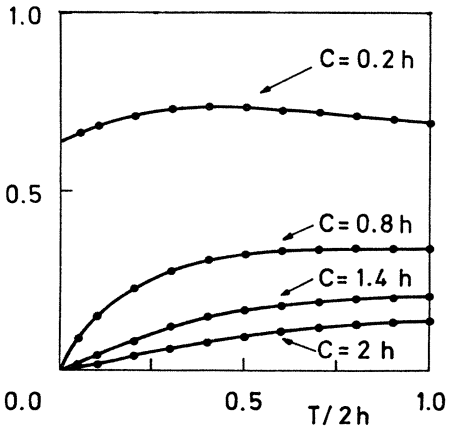

FIG. 11. The solid line shows the temperature dependence of the mean effective tunneling rate λ [cf. Eqs. (4.3a), (4.3b), (4.5a), and (4.5b)] for several values of the coupling C. The phonon cutoff frequency $\omega_D/2h=0.2$.

In Fig. 11, we have plotted λ given by (4.5b) as a function of temperature for several values of C. Our results indicate that λ goes to zero as $T\to 0$ when the coupling constant is above the critical value. Thus we see that in the strong-coupling regime the periodicity of the tunneling process is completely lost. Nevertheless, tunneling still occurs, but the process is stochastic instead of periodic, and the effective tunneling rate is given by λ. The vanishing of the effective tunneling rate as $T\to 0$ implies that the ergodicity of the system is lost, and that the spin is effectively confined to one of the states $|\uparrow\rangle$ or $|\downarrow\rangle$. Here we must mention that we are not able to provide definite results for the system in its ground state. Our statements are based on results for finite, though very low, temperatures. However, the question of whether the time during which the system is confined to a certain region of phase space is very long or really infinite becomes irrelevant, when this time is much longer than the duration of experiments.[20]

The only theory allowing for a direct quantitative comparison with ours is that of Beck *et al.*[5] who have used a mode-coupling theory to calculate both the static and dynamic properties of the two-level system. Some of their results for the static functions have been reproduced in Figs. 4–6.[21] For weak coupling ($C/2h\lesssim 0.2$) their results are in good qualitative agreement with ours. For intermediate coupling $C/2h\approx 0.4$, deviations from our results clearly show up. In particular, the mode coupling fails to reproduce $\langle\sigma^x\rangle$ and χ^x if $C/2h>0.2$. The mode-coupling scheme breaks down for strong coupling.

So far we have considered the case where the system resembles the adiabatic model because we have taken $\omega_D=\max(\omega_k)$ rather small ($\omega_D/2h=0.2$). We now investigate the effect of increasing $\omega_D/2h$ such that there are more oscillator modes that fall outside the adiabatic regime. Strictly speaking, $\omega_D/2h\to 0$ is not equivalent to taking the adiabatic limit but operationally we can recover the adiabatic result from the path-integral representation if we let $\omega_D/2h\to 0$. If $\omega_D/2h$ increases, the wave-vector dependence of the phonon spectrum and the coupling become important. In particular the similarity between the 1D and 3D results that was found for small $\omega_D/2h$ is lost. In the remainder of this section we will confine the discussion to the 1D phonons because we have studied this model in much more detail than the 3D case.

A feeling for the importance of the nonadiabatic contributions is obtained by studying the limiting form ($m\to\infty$) of $F(\alpha)$, as given by [(2.10) and (2.11)]. For phonons and coupling given by (3.1) or (3.2) we evaluate $F(\alpha)$ by first performing the integration over k analytically and summing numerically over γ in (2.11) afterwards. Replacing the wave-vector sum by an integral means that we have taken the thermodynamic limit $N\to\infty$ first. For a given choice of ω_D and T we then increased m until convergence was achieved. Obviously $\lim_{m\to\infty}F(\alpha)$ does not depend on ω_D *and* T, but only on the ω_D/T. We considered values of $\omega_D/T\lesssim 10^5$. The

convergence of the long-range part of $F(\alpha)$ is very fast, and even for $\omega_D/T=10^5$, $m=100$ is sufficient to obtain three-digit accuracy. The convergence rate of the short-range part of $F(\alpha)$, however, decreases rapidly when ω_D/T increases. Although (3.1) does not describe Debye phonons we found that $\lim_{m\to\infty}F(\alpha)$ can be fitted very well by $\sin^{-2}(\pi\alpha/m)$, which is precisely the form appearing in the effective action derived by Bray and Moore.[22] Note that Bray and Moore, in order to be able to use the renormalization-group treatment, replace the sine by its argument, thus getting a $(\alpha/m)^{-2}$ interaction. Whereas this is valid for $\alpha\ll m$, this replacement may influence the final results significantly. It is easy to check that the long-range behavior of the effective interaction of the original model of Bray and Moore, and thus also our model, differs considerably from an inverse-square interaction.

An alternative way to obtain a $(\alpha/m)^{-2}$ interaction is to take the $m\to\infty$ limit in (2.11) first [which results in (2.22b)], then taking the low-temperature limit of (2.22b) yielding $I_k(\alpha)=\exp(-\tau\omega_k\,|\,\alpha\,|\,m)$, and then performing the integration over k in (2.10). Obviously this procedure is legitimate only if $\min(\omega_k)>0$ and the temperature is very small compared to $\min(\omega_k)>0$. The Fröhlich polaron is an example where these conditions are satisfied and where excellent results for the ground-state properties were obtained in this way.[23] In the case of the two-level system, however, where the $k\approx 0$ acoustic phonons are responsible for the transition between a quasi-free and self-trapped state, a proper treatment of these low-frequency modes is essential. To conclude this discussion, we find that there is no legitimation for replacing the real effective interaction by an inverse-square interaction for any nonzero temperature regardless of how large ω_D may be. Although an inverse-square model is interesting on its own, there is no proof that it is relevant for the two-level system.

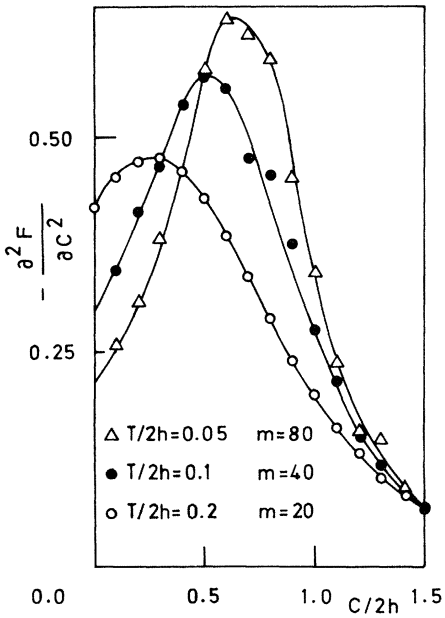

FIG. 12. Coupling dependence of the fluctuation of the coupling energy [cf. Eq. (2.19)] for different temperatures and for a constant value of the "imaginary time step" $\tau=\beta/m$. Data for $m=20$ are exact. Data for $m=40$ and 80 are from Monte Carlo simulations. The phonon cutoff frequency $\omega_D/2h=2$.

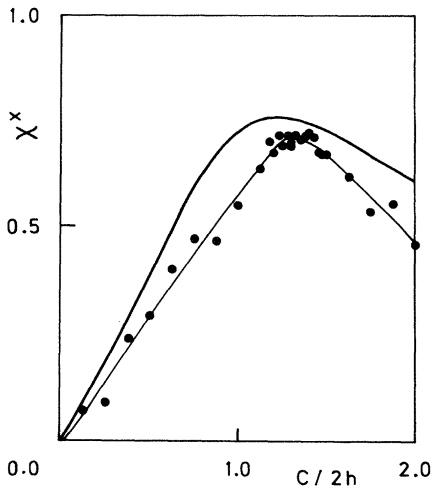

FIG. 13. Coupling dependence of χ^x for $\omega_D/2h=5$. The thick solid line represents exact results for $T/2h=0.1$ and $m=20$. The dots are Monte Carlo results for $T/2h=0.025$ and $m=160$. The thin line serves as a guide to the eye only.

We have made extensive numerical calculations for $\omega_D/2h=2$, 5, 10 for different temperatures and m values. The results are summarized in Figs. 12–16. From these data we have drawn the following conclusions. By increasing $\omega_D/2h$ the transition from the quasi-free to the self-trapped state becomes less abrupt and the critical value of the coupling, which according to the adiabatic limit is defined by the coupling ($C_{\max}$) at which $-\partial^2F/\partial C^2$ reaches a maximum, increases. Of course, if the transition becomes smoother it also becomes harder to

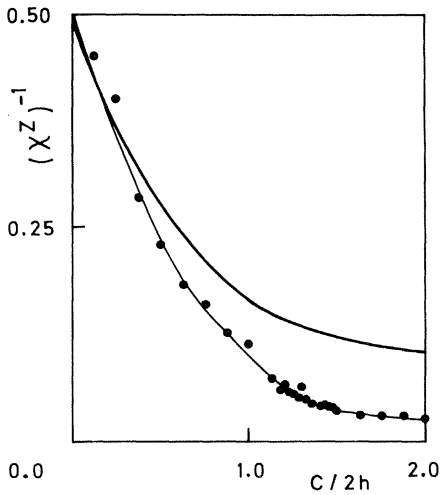

FIG. 14. Coupling dependence of $(\chi^z)^{-1}$ for $\omega_D/2h=5$. The thick solid line represents exact results for $T/2h=0.1$ and the number of products in the Trotter formula $m=20$. The dots are Monte Carlo results for $T/2h=0.025$ and $m=180$. The thin line serves as a guide to the eye only.

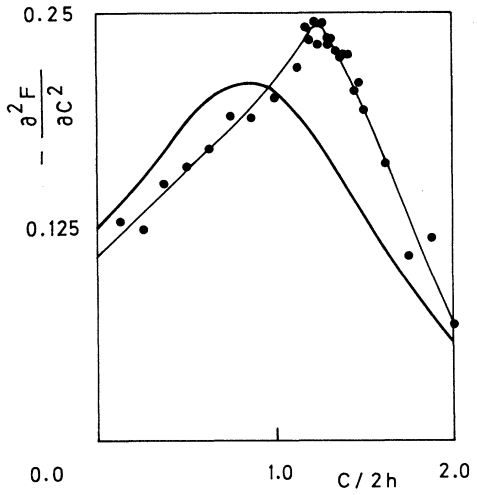

FIG. 15. Coupling dependence of the fluctuations of the coupling energy for $\omega_D/2h=5$. The thick solid line represents exact results for $T/2h=0.1$ and $m=20$. The dots are Monte Carlo results for $T/2h=0.025$ and $m=160$. The thin line serves as a guide to the eye only.

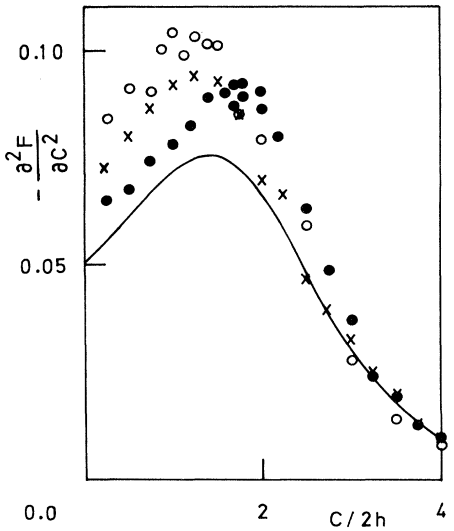

FIG. 16. Coupling dependence of the fluctuation of the coupling energy for $\omega_D/2h=10$. The thick solid line represents exact results for $T/2h=0.1$ and $m=20$. The crosses and open circles are Monte Carlo results for the same temperature $T/2h=0.1$, but for $m=40$ and 80, respectively. The solid dots are Monte Carlo results for $T/2h=0.05$ and $m=80$.

determine the critical value of the coupling constant accurately. For this reason we decided that it did not make much sense to go to still larger $\omega_D/2h$. The dependence of the peak position of $-\partial^2 F/\partial C^2$ (an estimate for the critical coupling) on $\omega_D/2h$ suggests that $C_{\max}/\omega_D$ goes to a constant if $\omega_D \to \infty$, in qualitative agreement with the renormalization-group[22,24] and mode-coupling[25] $C_{\max}/\omega_D=\pi/8$ prediction. Although there is a considerable shift of the maximum of $-\partial^2 F/\partial C^2$ as a function of temperature, we believe that it is unlikely that this shift can account for the observed quantitative discrepancy. This is due to difference in behavior of $F(\alpha)$, as discussed above.

Unlike the renormalization-group treatment which only seems to yield an estimate for the "renormalized" tunneling frequency the mode-coupling theory[25] gives information about most physical properties of interest. It would be interesting to see to what extent the recent mode-coupling calculations[25] reproduce our numerical data for the static properties in order to evaluate the accuracy of this approximation scheme on a quantitative basis.

As far as dynamics is concerned we conclude that in the strong-coupling regime the inverse relaxation time (λ) is proportional to T, independent of the particular value of $\omega_D/2h$. This follows directly from the temperature dependence of the frequency moments which is essentially the same as for $\omega_D/2h=0.2$. The temperature dependence of the relaxation rate is determined by χ^z since $\chi^z \sim T^{-1}$ and all other quantities that appear in the expressions of the frequency moments are slowly varying functions of T. Of course the temperature dependence of the relaxation rate is more or less determined by the assumption that the relaxation function decays exponentially in time (this assumption was also made in Ref. 22).

To summarize, we find that the main effect of increasing $\omega_D/2h$ is to smear out the transition from the quasi-free to the self-trapped state and to increase the value of the coupling at which this transition occurs. For the parameter range covered we conclude that there is no notable qualitative change in the spin properties (magnetization and susceptibilities) if $\omega_D/2h$ changes.

ACKNOWLEDGMENTS

We thank W. Götze for discussions and useful suggestions and for drawing our attention to existing work on this subject. We are grateful to A. J. Bray and M. A. Moore for clarifying remarks on their work and for pointing out several shortcomings and incorrect statements in the previous version of the manuscript. The authors thank the National Fund for Scientific Research Belgium for financial support. This work was supported by the Inter University Institute for Nuclear Sciences Belgium.

[1]T. Holstein, Ann. Phys. (N.Y.) 8, 343 (1959).
[2]H. B. Shore and L. M. Sander, Phys. Rev. B 7, 4537 (1973).
[3]N. Rivier and T. J. Coe, J. Phys. C 10, 4471 (1977).
[4]P. Prelovsek, J. Phys. C 12, 1855 (1979).
[5]R. Beck, W. Götze, and P. Prelovsek, Phys. Rev. A 20, 1140 (1979).
[6]R. Pirc and J. A. Krumhansl, Phys. Rev. B 11, 4470 (1975).
[7]H. B. Shore and L. M. Sander, Phys. Rev. B 12, 1546 (1975).
[8]W. Press, *Single-Particle Rotations in Molecular Crystals, Springer Tracts in Modern Physics No. 92* (Springer, Berlin, 1981).
[9]P. Pfeifer, Phys. Rev. A 26, 701 (1982).

[10]M. Blume, V. J. Emery, and A. Luther, Phys. Rev. Lett. 25, 450 (1970).
[11]V. J. Emery and A. Luther, Phys. Rev. B 9, 215 (1974).
[12]M. Suzuki, Commun. Math. Phys. 51, 183 (1976).
[13]M. Suzuki, Prog. Theor. Phys. 56, 1454 (1976).
[14]B. De Raedt and H. De Raedt, Phys. Rev. Lett. 50, 1926 (1983).
[15]K. S. Schweizer, R. M. Stratt, D. Chandler, and P. G. Wolynes, J. Chem. Phys. 75, 1347 (1981).
[16]K. Binder, *Monte Carlo Methods in Statistical Physics,* edited by K. Binder (Springer, Berlin, 1979).
[17]H. Mori, Prog. Theor. Phys. 34, 399 (1965).
[18]H. De Raedt and B. De Raedt, Phys. Rev. B 15, 5379 (1977).
[19]A. Abragam, *The Principles of Nuclear Magnetism* (Oxford University Press, Oxford, 1970).
[20]R. G. Palmer, Adv. Phys. 31, 669 (1982).
[21]In the work of Beck *et al.* the role of σ^x and σ^z is interchanged with respect to our definition. Further, the factor $\frac{1}{2}$ is included in their definition of σ^α. Thus their Ω corresponds with $2h$, Λ with $8C$, λ_k with $2B_k$, and χ^α with $\frac{1}{4}\chi^\alpha$.
[22]A. J. Bray and M. A. Moore, Phys. Rev. Lett. 49, 1545 (1982).
[23]R. P. Feynman, *Statistical Mechanics* (Benjamin, Reading, Massachusetts, 1976).
[24]This has been suggested to us by A. J. Bray and M. A. Moore (private communication).
[25]W. Zwerger, Z. Phys. B 53, 53 (1983).